Elastic Tube Subjected to Internal Detonation Pressure Loading

Fehmi Cirak

November 29, 2004

1 Problem description (Chao, Shepherd)

An *Al6061-T6* cylinder with dimensions

$$\begin{aligned} L &= 0.61 \quad m \\ R_{in} &= 0.01975 \quad m \\ R_{out} &= 0.02064 \quad m \\ t &= 0.00089 \quad m \end{aligned}$$

and material parameters

$$\begin{aligned} E &= 69 \cdot 10^9 \quad N/m^2 \\ \nu &= 0.33 \\ \rho &= 2780 \quad kg/m^3 \end{aligned}$$

is subjected to detonation loading (Fig. 1). The cylinder is modeled as a shell with a radius of $R = 0.020195m$ and a thickness of $t = 0.00089m$. The finite element discretizations consists of 16110 shell finite elements.

2 Detonation pressure loading

The detonation pressure loading on the cylinder can be approximated with the Taylor-Zeldovich model:

$$p(x,t) = \begin{cases} p_1, & 0 < t < t_{cj} \\ (p_2 - p_3)e^{(t_{cj}-t)/T}) + p_3, & t_{cj} < t < \infty \end{cases} \tag{1}$$

with

$$t_{cj} = x/v_{cj}$$

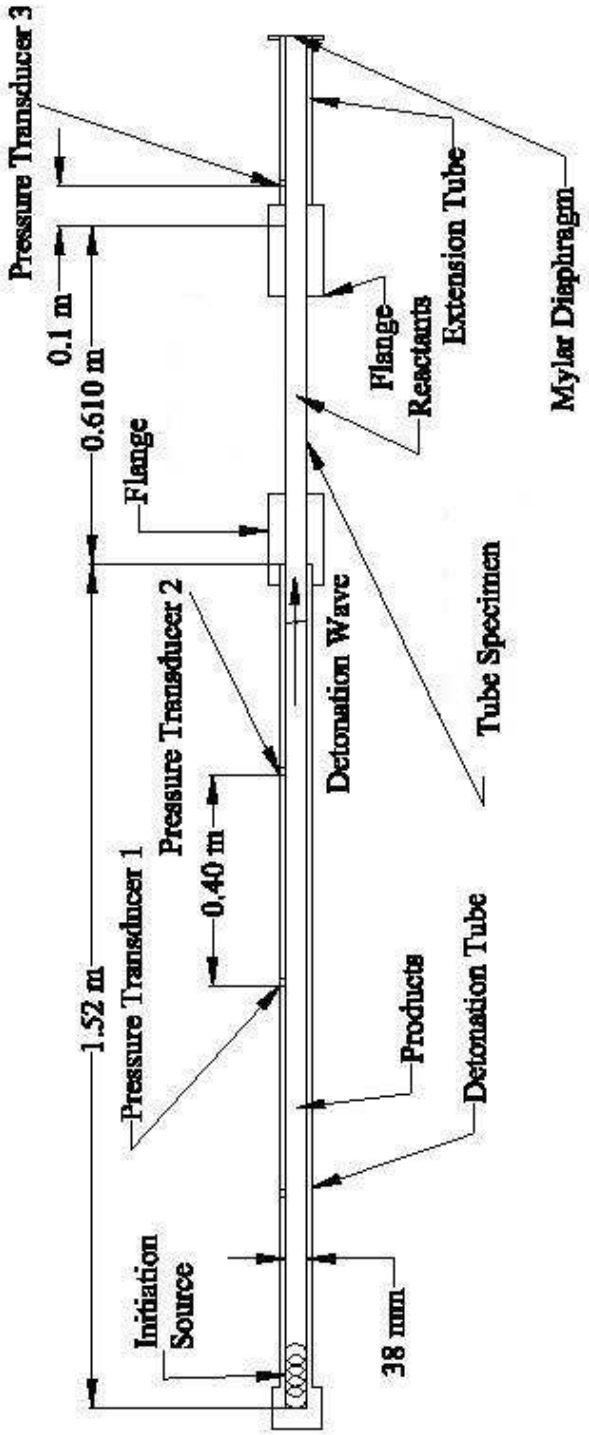

Figure 1: Experimental set up [2].

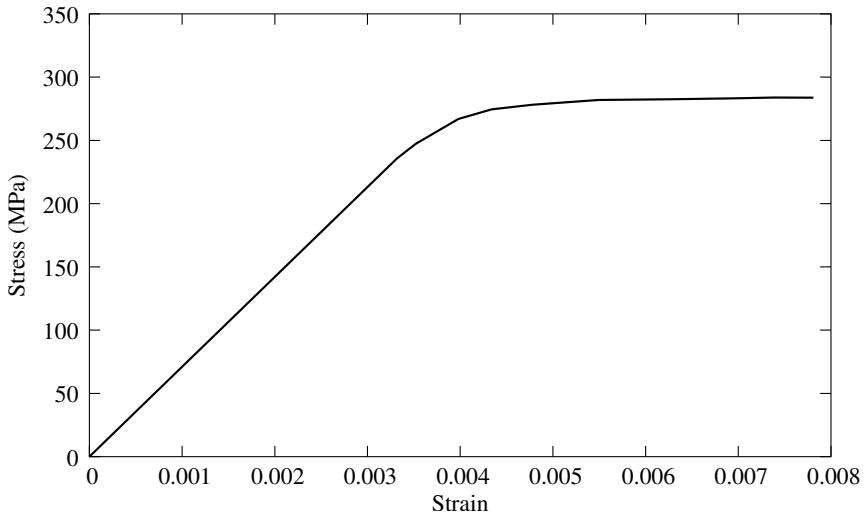

Figure 2: Stress-strain plot for Al6061-T6.

and

$$T \approx t_{cj}/3. \tag{2}$$

For the numerical computations following parameters have been chosen:

$$\begin{aligned} p_1 &= 0.0 \quad Pa \\ p_2 &= 2.6 \cdot 10^6 \quad Pa \\ p_3 &= 0.75 \cdot 10^6 \quad Pa \\ v_{cj} &= 2365.0 \quad m/s \end{aligned}$$

The comparison between the experimental and approximated pressure plots are shown in Figures 3 and 4.
The sound speed in aluminum is:

$$v_{cyl} = \sqrt{\frac{E}{\rho(1-\nu^2)}} = 5277.6 \quad m/s \tag{3}$$

The transversal wave speed of the tube is:

$$v_{c0,cyl} = \left[\frac{E^2 h^2}{3\rho^2 R^2 (1-\nu^2)}\right]^{1/4} = 813.46 \quad m/s \tag{4}$$

The shear wave speed in aluminum is:

$$v_{d,cyl} = \sqrt{\frac{\kappa G}{\rho}} = \sqrt{\frac{\kappa E}{2.0 \cdot (1.0+\nu)\rho}} = 2788.5 \quad m/s \tag{5}$$

with $\kappa = \frac{5}{6}$

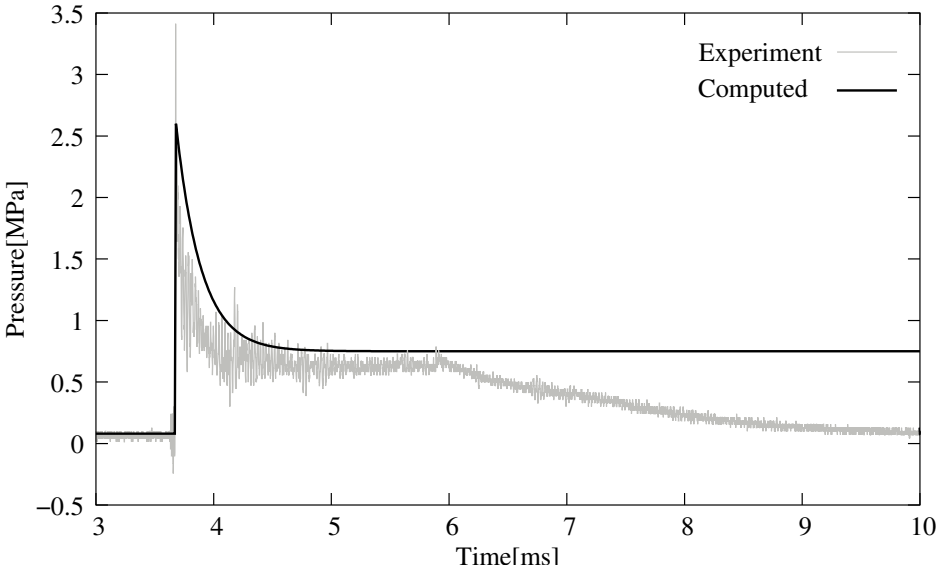

Figure 3: Experimental pressure history and its approximation at transducer 1.

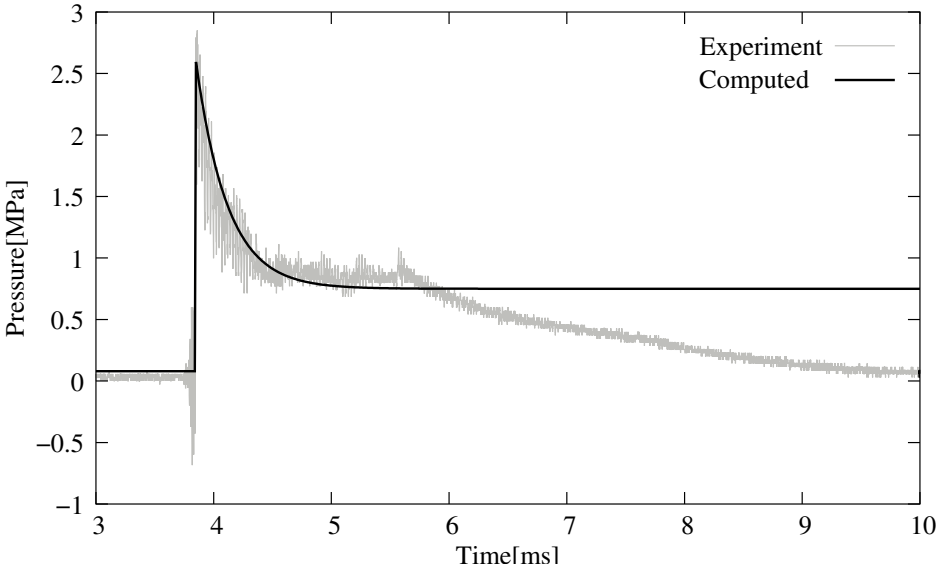

Figure 4: Experimental pressure history and its approximation at transducer 2.

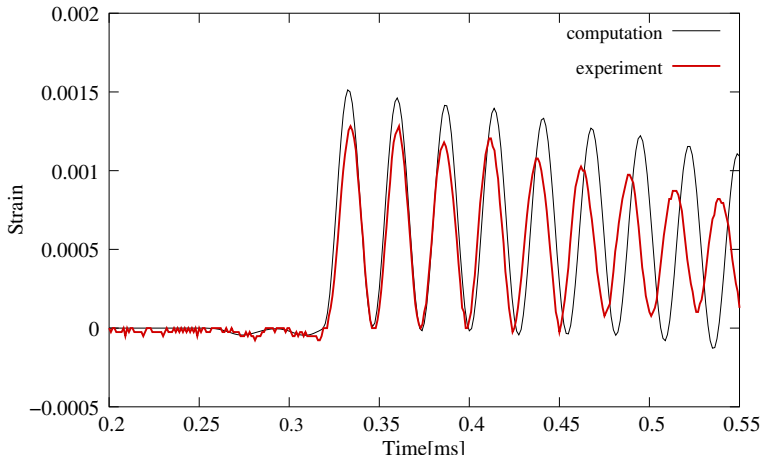

Figure 5: Geometrically perfect tube. Comparison of circumferential strain at gage one at 282 mm.

3 Comparison of the experiment with thin-shell computations

3.1 Geometrically perfect tube

Strain Gage Locations: Strain gages one, two, and four are located along an axial line on the outer tube surface at 282 mm, 297 mm, and 328 mm from the left end of the specimen. Strain gage 6 is located at 180^o at 305 mm.

3.2 Tube with thickness imperfections

We assume a thickness imperfection of five or ten percent ($E = 5$ or $E = 10$ in Fig. 7). The computed circumferential strain has been plotted at the five positions shown in Fig. 7, right. The results for an elastic tube with a thickness imperfection of five percent and a thickness of 0.00089, 0.0008, and 0.00098 are plotted in Figs. 8, 10, and 11, respectively.

The results for an elastic tube with a thickness imperfection of ten percent and a thickness of 0.00089 is plotted in 9.

The results for a viscoplastic tube with a thickness imperfection of ten percent, a thickness of 0.00089, and a yield stress of $\sigma_y = 90MPa$ or $\sigma_y = 50MPa$ are plotted in Figs. 12 and 14 , respectively.

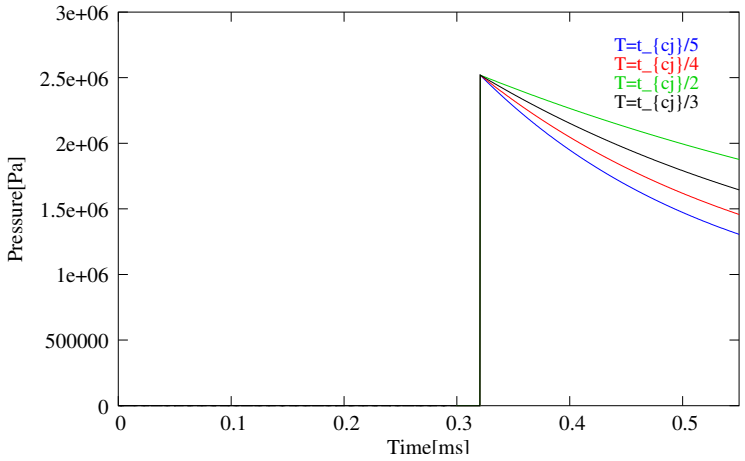

Figure 6: Computational pressure at strain gage one at 282 mm for different exponential decay rates (see equation 2).

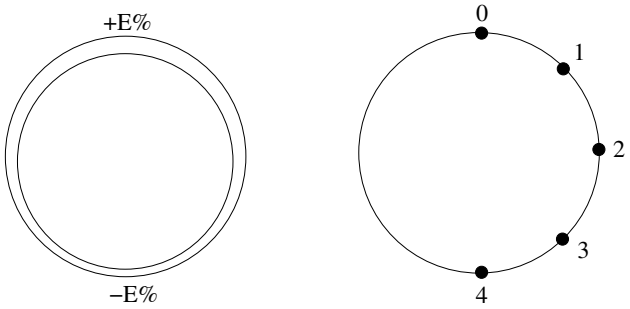

Figure 7: Tube with thickness imperfection and computational sensor positions.

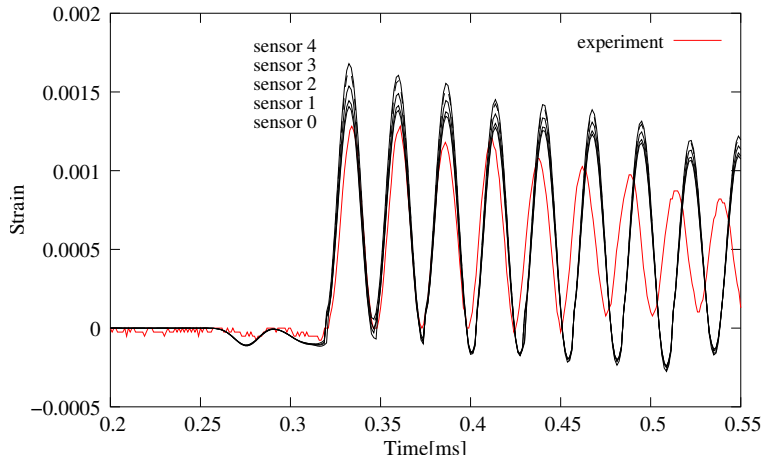

Figure 8: Tube with 5% thickness imperfection and $t = 0.00089m$. Comparison of the circumferential strain at $0.282m$.

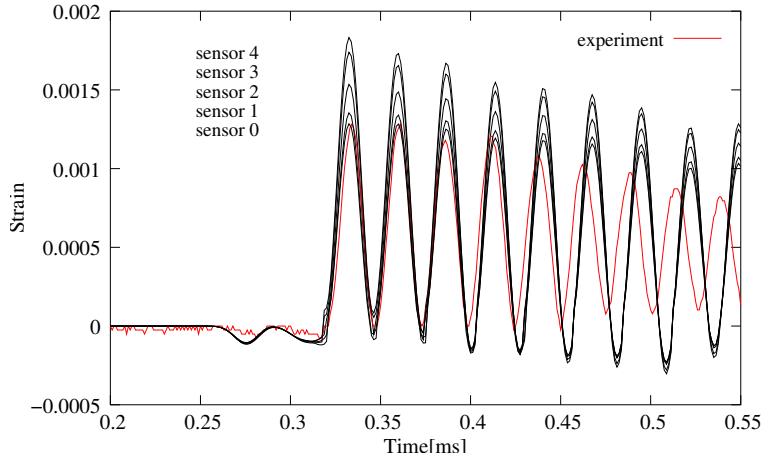

Figure 9: Tube with 10% thickness imperfection and $t = 0.00089m$. Comparison of the circumferential strain at $0.282m$.

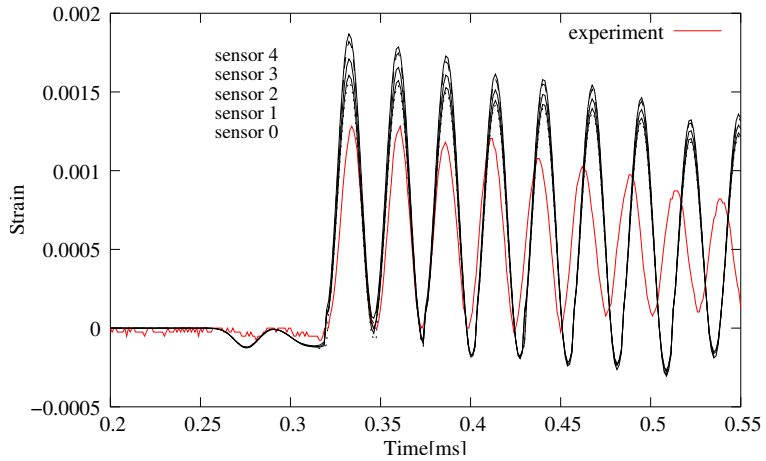

Figure 10: Tube with 5% thickness imperfection and $t = 0.0008m$. Comparison of the circumferential strain at $0.282m$.

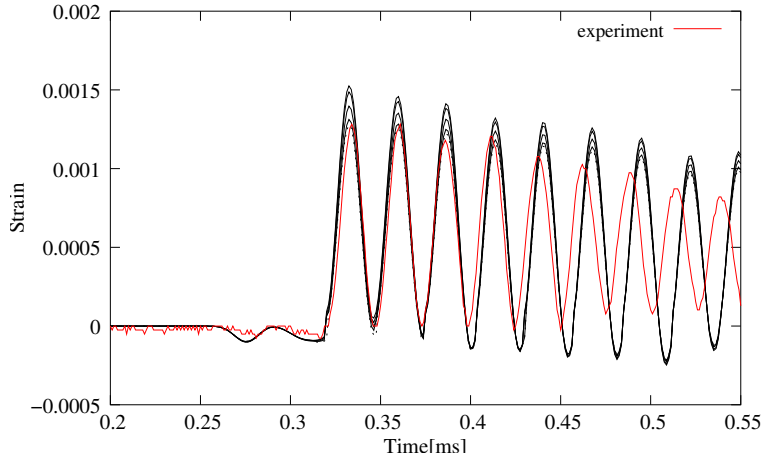

Figure 11: Tube with 5% thickness imperfection and $t = 0.00098m$. Comparison of the circumferential strain at $0.282m$.

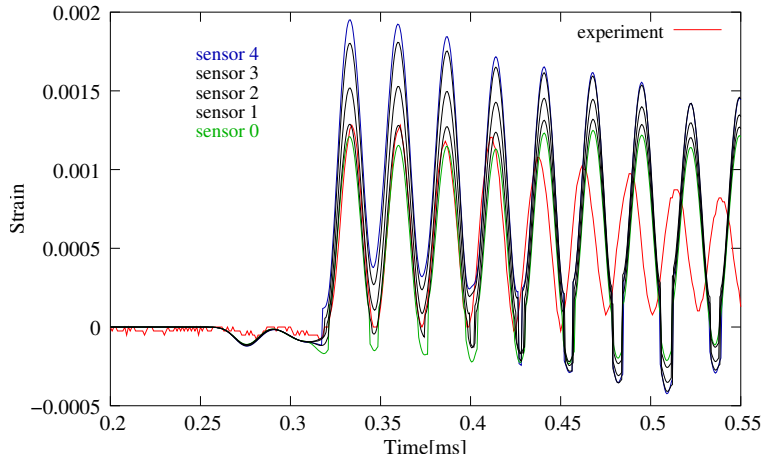

Figure 12: Tube with 10% thickness imperfection, $t = 0.00089m$, and $\sigma_y = 90MPa$. Comparison of the circumferential strain at $0.282m$.

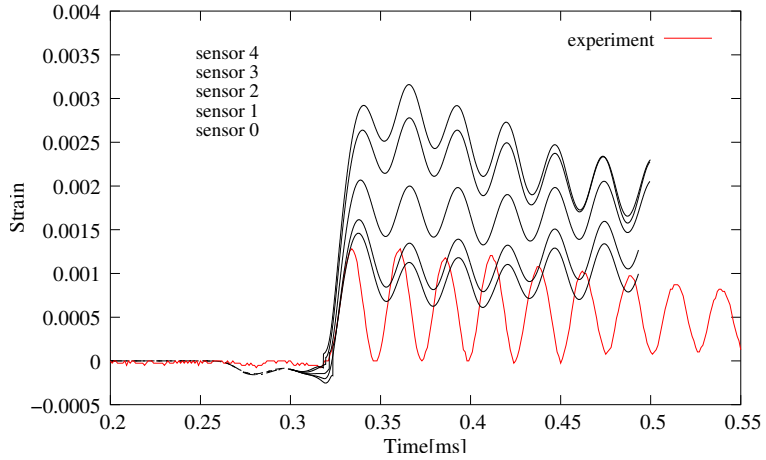

Figure 13: Tube with 10% thickness imperfection, $t = 0.00089m$, and $\sigma_y = 50MPa$. Comparison of the circumferential strain at $0.282m$.

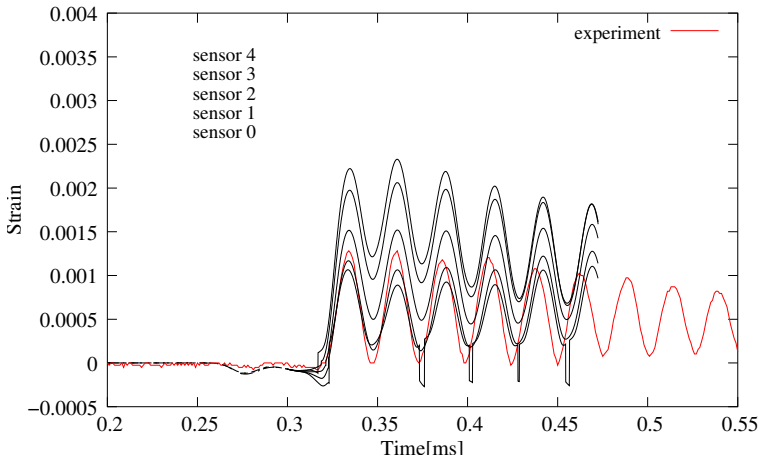

Figure 14: Tube with 12% thickness imperfection, $t = 0.00089m$, and $\sigma_y = 70MPa$. Comparison of the circumferential strain at $0.282m$.

3.3 Sensitivity to detonation parameters

The results are plotted in Figures 15 and 16.

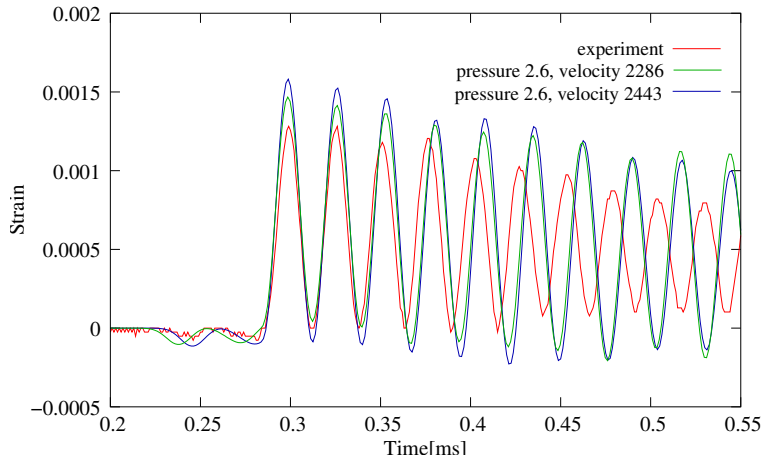

Figure 15: CJ velocities $2286m/s$ and $2443m/s$. Comparison of the circumferential strain at $0.282m$.

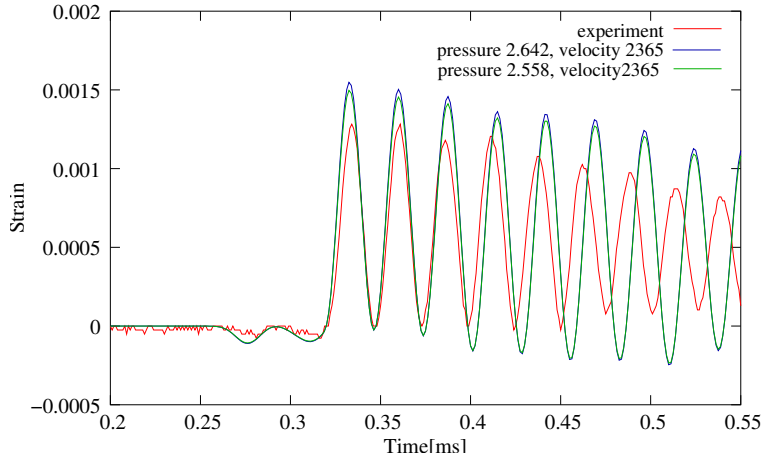

Figure 16: CJ pressures $2.642MPa$ and $2.558MPa$. Comparison of the circumferential strain at $0.282m$.

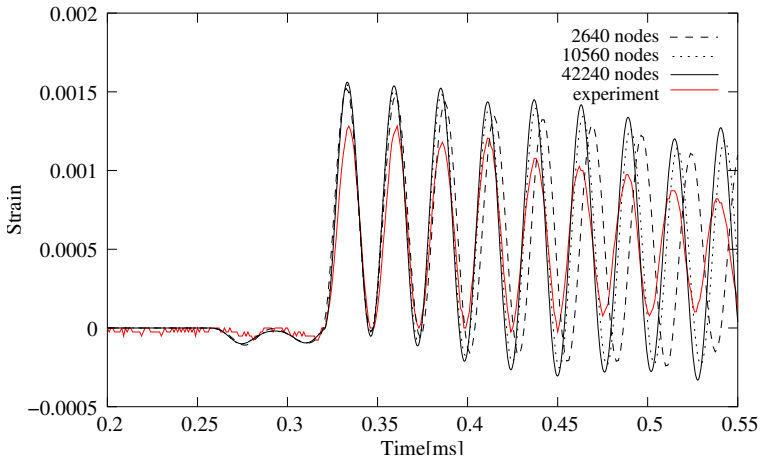

Figure 17: Three different meshes. Comparison of the circumferential strain at $0.282m$.

3.4 Sensitivity to mesh size

The results for three different meshes with 2640, 10560, and 42240 nodes are plotted in Figure 17.

The element size necessary to resolve the occurring vibrations can be estimated from the wave length

$$\lambda \approx \frac{813.46\frac{m}{s}}{39000.0s} = 0.021m. \tag{6}$$

Hence, the element length should be less than $0.021/20m \approx 0.0011m$. The total number of nodes can be estimated with

$$\frac{2.0 \cdot 3.14 \cdot 0.020195}{0.0011} \cdot \frac{0.61}{0.0011} = 115.3 \cdot 554.5 = 63933.8 \tag{7}$$

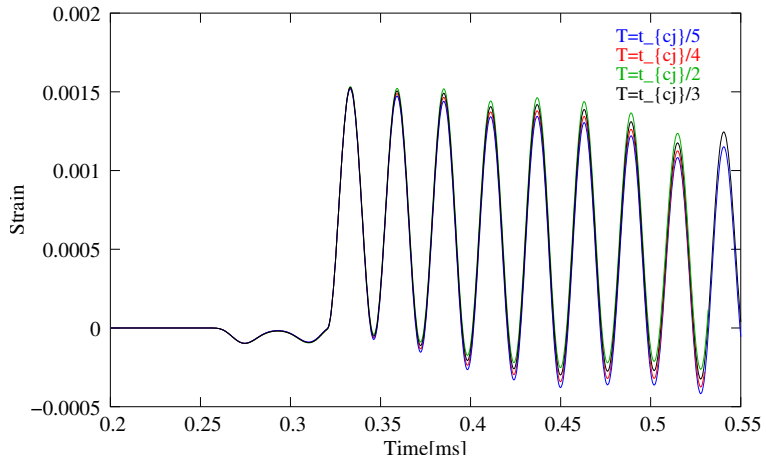

Figure 18: Comparison of the circumferential strain at $0.282m$ for three different pressure decay rates (see equation 2 and figure 6).

4 Sensitivity to pressure decay rate

The results for three different pressure decay rates (see figure 6) are plotted in figure 18. The mesh size for all three computations is 42240 nodes.

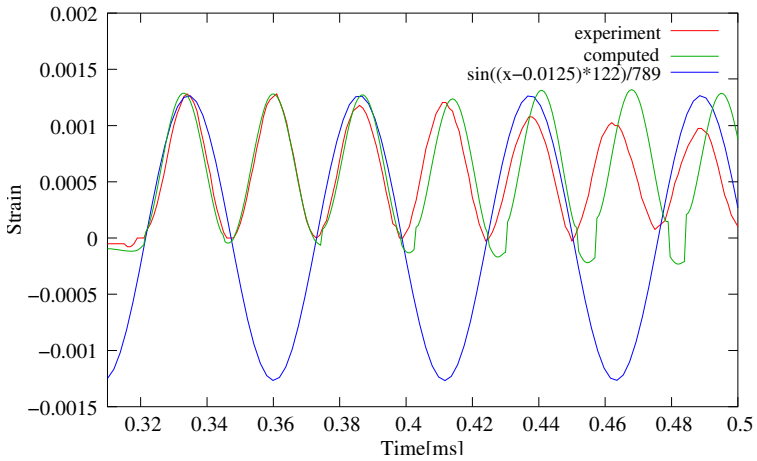

Figure 19: Circumferential strains for the experiment and computation compared with a sinus wave of $19417Hz$.

5 Mass spring model

The experimental tube vibrates with a frequency of $2 \times 19417Hz = 38294.0Hz$ (see Fig. 19). The frequency of the damped computational tube is slightly smaller.

An analytical estimate for the tube frequency can be derived by considering a small piece of the tube with the dimensions $[ds \times t \times 1]$ as attached to a spring with the stiffness c. For a ring, the following relation between the internal pressure p and radial displacements Δr is valid:

$$p = \frac{Et}{r^2}\Delta r \tag{8}$$

Hence, the tube can be represented by a mass spring model with:

$$t\rho\Delta\ddot{r} \quad ds + \frac{Et}{r^2}\Delta r \quad ds = 0 \tag{9}$$

The frequency of the mass spring model

$$f = \frac{1}{2\pi}\sqrt{\frac{E}{r^2\rho}} = 39282\frac{1}{s} \tag{10}$$

is in good agreement with the measured tube frequency.

The mass spring model should give a good estimate for the maximum displacements during the dynamic pressure loading, since

- the transversal wave speed in the tube is by a factor of $2365/813.5 = 2.907$ smaller than the detonation velocity

- the pressure can be assumed constant during one cycle, $T = 1/f = 0.02545ms$ (see Fig. 6)

Using these assumptions and energy conservation, the circumferential strain in the dynamically loaded tube can be estimated with:

$$\epsilon = \frac{2pr}{Et} = 0.001616 \tag{11}$$

which is in good agreement with the computations.

Note, in the previous derivations only the "ring" stiffness has been considered. Therefore, the computed quantities can be considered as upper bounds for the experimental values.

6 Normal shock equations

For an ideal gas the following relations between the unshocked x_1 and shocked x_2 state variables are valid:

$$\frac{p_2}{p_1} = \frac{2\gamma M_1^2 - (\gamma - 1)}{\gamma + 1} \tag{12}$$

$$\frac{\rho_2}{\rho_1} = \frac{(\gamma + 1)M_1^2}{(\gamma - 1)M_1^2 + 2} \tag{13}$$

$$\frac{T_2}{T_1} = \frac{[2\gamma M_1^2 - (\gamma - 1)][(\gamma - 1)M_1^2 + 2]}{(\gamma + 1)^2 M_1^2} \tag{14}$$

where M_1 is the shock Mach number defined as

$$M_1 = \frac{W_s}{a_1} \tag{15}$$

where W_s is the shock velocity relative to the tube and a_1 is the sound speed in the unshocked gas, given by:

$$a_1^2 = \frac{\gamma p_1}{\rho_1} \tag{16}$$

In the present experiment, the ratio of the CJ pressure $2.6 \cdot 10^6$ to the unshocked pressure $80 \cdot 10^3$ requires a shock with $M_1 = 5.2915$. Further, the CJ shock velocity of 2365 gives a unshocked density of 0.5607, which leads to a shocked density of 2.85441. The velocity in the shocked region is initialized with 1900.5 and in the unshocked region with 0.

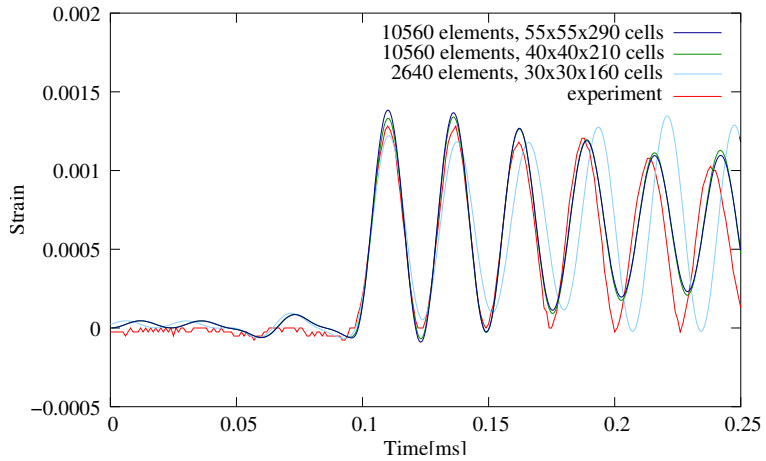

Figure 20: Comparison of the circumferential strain at $0.282m$.

7 Shell-Fluid Coupled Simulation

Initial conditions in the shocked region are

$$\rho = 6.9078 \quad p = 2.0 \cdot 10^6 \quad w = 2144.56 \tag{17}$$

and in the unshocked region are

$$\rho = 1.0121, \quad p = 8.0 \cdot 10^4 \quad w = 872.13 \tag{18}$$

The frequency of the tube vibrations for the used coarse shell mesh is smaller than the experimental frequency, Fig. 20.

8 Shell - 1D Full Chemistry Coupled Simulation

The shell is discretized with 84288 elements. The pressures have been computed using a full chemistry model for the gaseous detonation of the ethylene oxygen mixture. Fig. 21.

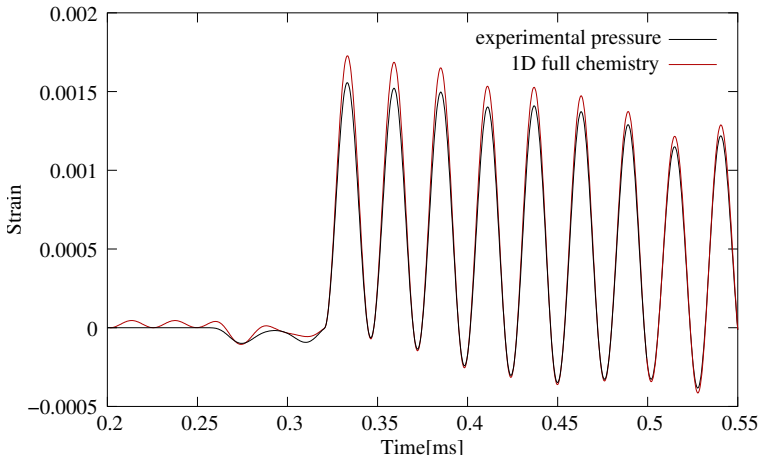

Figure 21: Comparison of the circumferential strain at $0.282m$.

References

[1] W. Beltman and J.E. Shepherd. Linear elastic response of tubes to internal detonation loading. *Journal of Sound and Vibration*, 252(4):617–655, 2002.

[2] T.W. Chao and J.E. Shepherd. Fracture response of externally-flawed cylindrical shells to internal gaseous detonation loading. In *ASME Pressure Vessels and Piping Conference*, number PVP2002-1491, August 2002.